

Highly ionized absorbers at high redshift

Jacqueline Bergeron¹ and Stéphane Herbert-Fort¹

¹Institut d’Astrophysique de Paris-CNRS, 98bis Boulevard Arago, F-75014, Paris, France
 email: bergeron@iap.fr

Abstract. We build a sample of O VI absorption systems in the redshift range $2.0 \lesssim z \lesssim 2.6$ using high spectral resolution data of ten quasars from the *VLT-UVES* Large Programme. We investigate the existence of a metal-rich O VI population and define observational criteria for this class of absorbers under the assumption of photoionization. The low temperatures of nearly half of all O VI absorbers, implied by their line widths, are too low for collisional ionization to be a dominant process. We estimate the oxygen abundance under the assumption of photoionization; a striking result is the bimodal distribution of [O/H] with median values close to 0.01 and 0.5 solar for the metal-poor and metal-rich populations, respectively. Using the line widths to fix the temperature or assuming a constant, low gas density does not drastically change the metallicities of the metal-rich population. We present the first estimate of the O VI column density distribution. Assuming a single power-law distribution, $f(N) \propto N^{-\alpha}$, yields $\alpha \sim 1.7$ and a normalization of $f(N) = 2.3 \times 10^{-13}$ at $\log N(\text{O VI}) \sim 13.5$, both with a $\sim 30\%$ uncertainty. The value of α is similar to that found for C IV surveys, whereas the normalization factor is about ten times higher. We use $f(N)$ to derive the number density per unit z and cosmic density, $\Omega_b(\text{O VI})$, selecting a limited column density range not strongly affected by incompleteness or sample variance. Comparing our results with those obtained at $z \sim 0.1$ for a similar range of column densities implies some decline of dn/dz with z . The cosmic O VI density derived from $f(N)$, $\Omega_b(\text{O VI}) \approx (3.5 \pm 3.2) \times 10^{-7}$, is 2.3 times higher than the value estimated using the observed O VI sample (of which the metal-rich population contributes $\sim 35\%$), easing the problem of missing metals at high z ($\sim 1/4$ of the produced metals) but not solving it. We find that the majority of the metal-rich absorbers are located within $\sim 450 \text{ km s}^{-1}$ of strong Ly- α lines and show that, contrary to the metal-poor absorbers, this population cannot be in hydrostatic equilibrium. All of the O VI absorber properties imply that there are two distinct populations: metal-poor absorbers tracing the intergalactic medium and metal-rich absorbers associated with active sites of star formation and most probably linked to galactic winds.

Keywords. quasars: absorption lines, intergalactic medium

1. Introduction

There are two major open questions that could be solved by the existence of a warm-hot and/or highly ionized phase of the intergalactic medium (IGM): the missing baryons at low redshift, $z \sim 0-0.5$, and the missing metals at $z \sim 2.5$.

The baryon budget at low z implies that about 45% of the cosmic baryons are still in the form of ionized gas in the IGM (Fukugita *et al.* 1998). The missing baryonic matter could reside in a warm-hot IGM (WHIM) as predicted by hierarchical structure formation models (see e.g. Cen & Ostriker 1999; Davé *et al.* 2001). The cooler phase of the WHIM can be probed by O VI $\lambda\lambda 1031, 1037$ absorption but, at the sensitivity of the *FUSE* and *HST* surveys, the contribution to the cosmic baryon density, Ω_b , of the detected O VI absorbers is only $\sim 5\%$ (Savage *et al.* 2002; Richter *et al.* 2004). The hotter phase of the WHIM, $T > 5 \times 10^5 \text{ K}$, can be probed by O VII-O VIII X-ray absorption. There are very few suitably bright targets for X-ray spectroscopy with *Chandra* and *XMM-Newton*, and the rare confirmed detections, at a significance level higher than 3σ (Nicastro *et al.*

2005a,b), have O VII column densities about ten times larger than those of O VI. The contribution of this intergalactic hot phase to Ω_b could be up to ten times higher than that of the cooler WHIM.

At $z \sim 2.5$, at least 90% of the baryons are in the Ly- α forest, but only about 10% of the metals produced by star formation activity in Lyman Break Galaxies (LBGs) have been detected up to now (Pettini 1999). The mean metal enrichment of the IGM could reach a value $Z \simeq 0.04 Z_\odot$ (Pettini 1999) and recent simulations of galactic winds give estimates in the range 0.01-0.06 Z_\odot (Bertone *et al.* 2005). The observed C IV cosmic density equals $\Omega_b(\text{C IV}) \sim 7 \times 10^{-8}$ (Songaila 2001; Scannapieco *et al.* 2005) and, assuming an ionization correction of about a factor two, leads to a cosmic abundance $[\text{C}/\text{H}] \sim -2.9$, thus a shortfall of metals by a factor of at least ten and maybe up to 10^2 . The missing metals could reside in hot gaseous halos around star-forming galaxies (Pettini 1999; Ferrara *et al.* 2005) and the cooler part of these hot bubbles might be traced by O VI absorption.

A few surveys of O VI absorbers at $z \sim 2.0\text{-}2.5$ have already been conducted at the *VLT* and *Keck* telescopes, some for only a limited number of sightlines (Bergeron *et al.* 2002; Carswell *et al.* 2002; Simcoe *et al.* 2002,2004). A non-negligible fraction, $\sim 1/3$, of the O VI absorptions associated with the Ly- α forest have line widths $b < 14 \text{ km s}^{-1}$, thus $T < 2 \times 10^5 \text{ K}$, which favors a radiative ionization process. A hard UV background flux, i.e. small discontinuity at 4 Ryd (Haardt & Madau 1996), reproduces well the observed ionic ratios for $-3.0 < [\text{Z}/\text{H}] < -0.5$. The inferred values of $\Omega_b(\text{O VI})$ of the above surveys are $\approx 1.1 \times 10^{-7}$ (assuming $\Omega_\Lambda, \Omega_m, \Omega_b, h = 0.7, 0.3, 0.04, 70$ throughout this paper). Applying a conservative ionization correction, O VI/O=0.15, yields a mean oxygen abundance of $[\text{O}/\text{H}] \sim -2.7$, and thus, as for C IV surveys, leaves open the problem of the missing metals.

However, a higher metallicity has been derived for O V absorbers. The EUV O V $\lambda 630$ singlet was searched for and detected in a stacked composite absorption spectra from *HST-FOS* data for absorbers at $1.6 < z < 2.9$ with a large range of H I column densities (Telfer *et al.* 2002). Except in the strongest H I systems, the lack of detection of the associated EUV O IV doublet also suggests a hard ionizing background flux, and the derived oxygen abundance is $[\text{O}/\text{H}] \sim -2.2$ to -1.3 .

The paper is organized as follows: our new *VLT* O VI sample is presented in § 2. In § 3, we give results on the oxygen abundance derived under various assumptions on the ionization process. The O VI column density distribution and the contribution of the O VI absorbers to the cosmic baryon density are given in § 4. The origin of these absorbers is discussed in § 5. We present our conclusions and prospectives in § 6.

2. The O VI sample

The *VLT-UVES* Large Programme “The Cosmic Evolution of the IGM” provides a homogeneous sample of quasar sightlines, with emphasis given to lower redshift quasars ($z < 3$) to take advantage of the high UV sensitivity of *UVES*. This allows a study of O VI systems in the range $z = 2.0\text{-}2.5$ where the crowding of the Ly- α forest is not too severe. Altogether, the sample comprises 21 bright quasars (most with $V < 17$), of which 19 are at $2 < z < 4$, observed with dichroics blue and red. The spectral resolution is $R = 45,000$ (line width $b = 6.6 \text{ km s}^{-1}$) and the exposure time per setting per quasar (2 settings per quasar) of 6 to 10 hr yields a signal-to-noise $\text{S/N} \sim 30\text{-}40$ and 100 at 3300 and 5500 Å respectively. The data were reduced using an upgraded version of the *ESO-UVES* data-reduction pipeline (Aracil *et al.* in preparation).

We present results derived from the spectral analysis of ten quasars at $2.1 < z_{em} < 2.8$. Our O VI sample comprises 136 absorbers with column densities in the range 12.7

$< \log N(O\text{VI}) < 14.6$. These absorbers span the redshift interval $1.99 < z < 2.57$ with a mean value of $\bar{z} = 2.28$. Due to partial blending of the associated H I absorptions and small velocity differences between the O VI and H I components, we group the O VI and H I absorptions into 51 systems. Absorption systems within 5000 km s^{-1} of the quasar emission redshift are excluded from this sample.

2.1. The O VI subsamples

There are unusual O VI absorbers with high abundances, $-1 < [\text{O/H}] \lesssim 0$, in previous O VI surveys (Bergeron *et al.* 2002; Carswell *et al.* 2002). They have high ionic ratios, $N(\text{O VI})/N(\text{H I}) > 0.5$, and low H I column densities, $\log N(\text{H I}) < 13.0$. The survey by Simcoe *et al.* (2004) focussed on systems with $\log N(\text{H I}) > 13.6$, which could account for the underrepresentation of highly metal-rich O VI absorbers in their O VI sample. Since these intriguing systems are not present in every sightline, a large quasar sample is mandatory for a statistically significant number of metal-rich O VI absorbers.

It is possible to define the class of metal-rich absorbers using observed column density ratios derived from photoionization models since the small line widths of a non-negligible fraction of the O VI systems imply “low” gas temperatures (see § 3.1). Adopting a hard UV background spectrum together with a 0.1 solar metallicity leads to observational identification criteria for the following classes of absorbers:

- type 1: $N(\text{O VI})/N(\text{H I}) > 0.25$: metal-rich absorbers,
- type 0: $N(\text{O VI})/N(\text{H I}) < 0.25$: metal-poor absorbers.

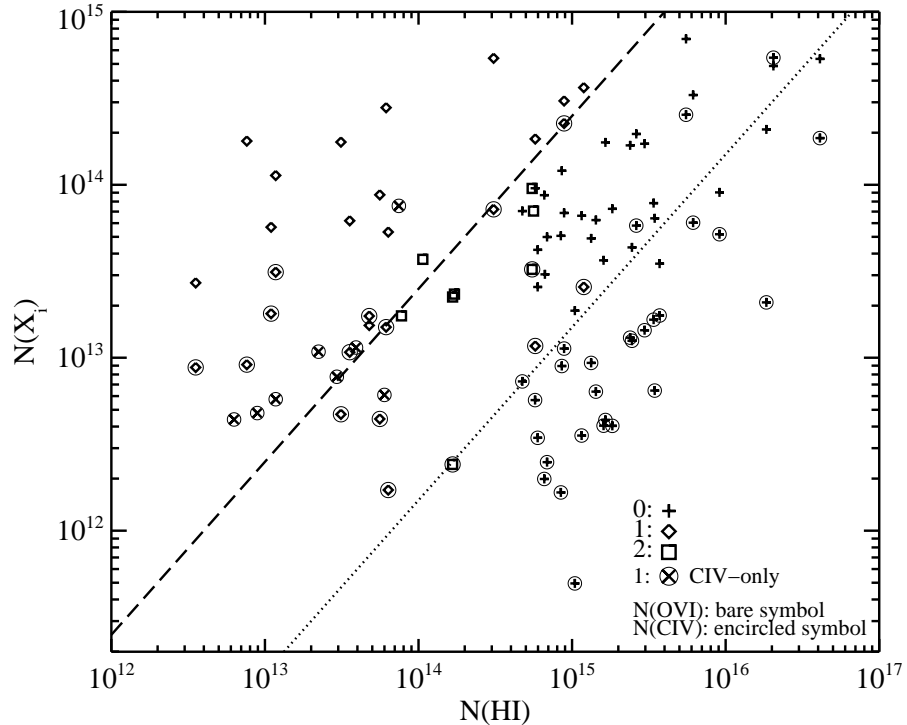


Figure 1. Metal column densities of O VI and C IV versus H I column density. The dashed and dotted line give the locations of systems with $N(\text{O VI})/N(\text{H I}) = 0.25$ and $N(\text{C IV})/N(\text{H I}) = 0.015$, respectively.

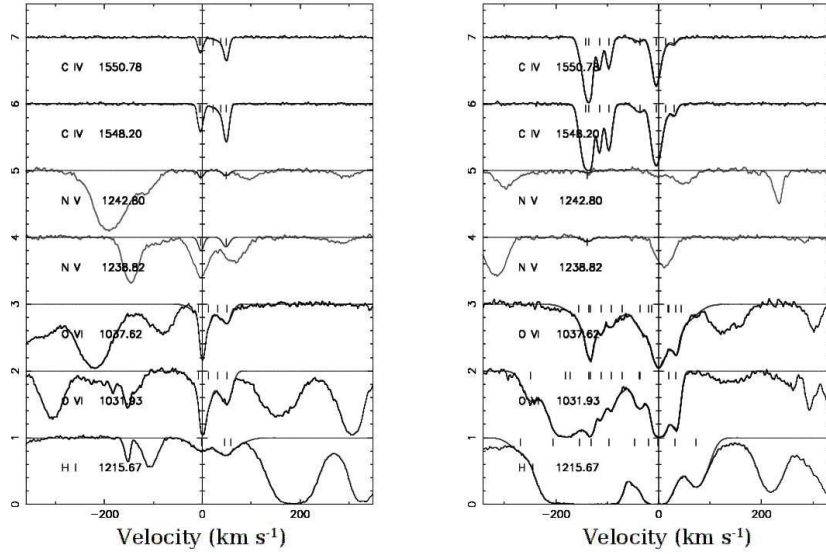


Figure 2. H I and metal absorptions of type 1 O VI absorbers: a weak H I system at $z = 2.468$ is shown in the left panel, and a strong H I system at $z = 2.398$ is shown in the right panel. The latter is 140 km s^{-1} away from a type 0 absorber.

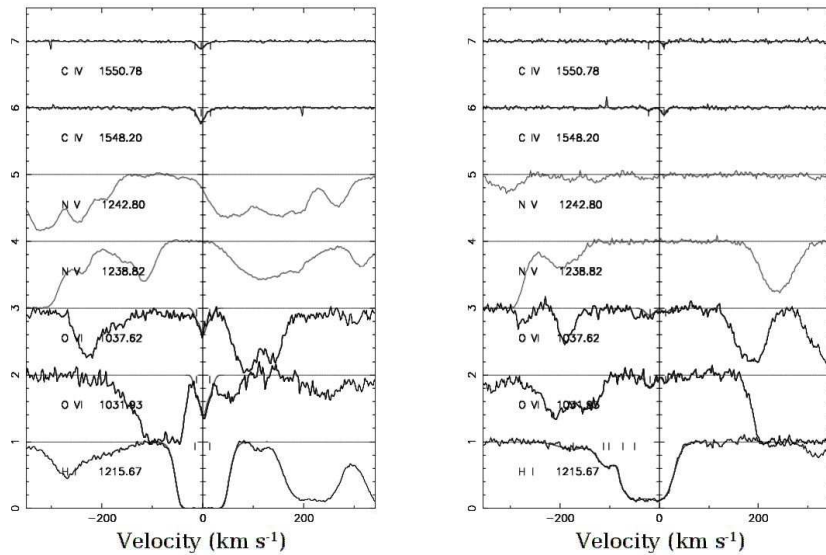


Figure 3. H I and metal absorptions of a type 0 O VI absorber at $z = 2.089$ (left panel) and a type 2 O VI absorber at $z = 2.314$ (right panel).

There are 39 O VI type 1 components, $12.9 < \log N(\text{O VI}) < 14.5$, grouped in 14 O VI-H I systems.

A similar criterium is derived for the C IV systems and is used to identify C IV-only

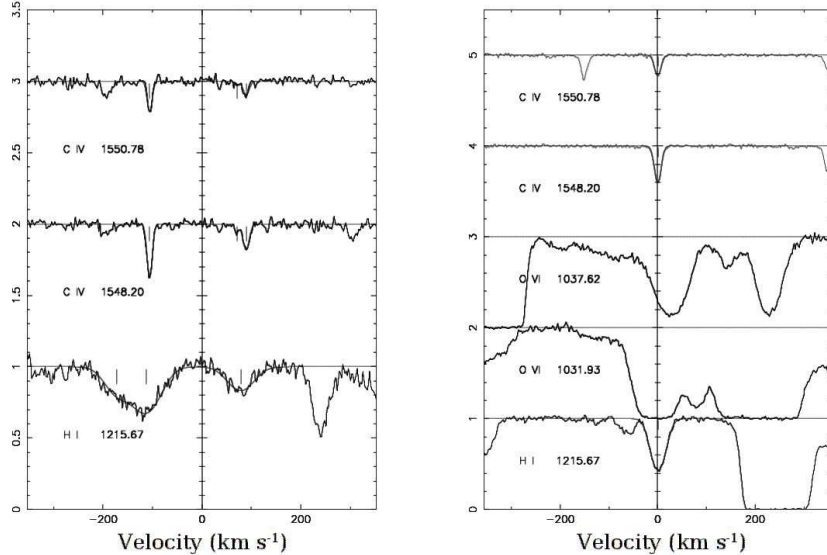


Figure 4. H I and metal absorptions of C IV-only type 1 absorbers: two low redshift systems at $z = 1.727$ and 1.729 (left panel) and one system at $z = 2.415$ with O VI lines fully blended with saturated Lyman lines (right panel).

metal-rich absorbers (O VI doublet either outside the observing range, $z < 2.0$, or fully blended with saturated Lyman lines):

- C IV-only type 1: $N(\text{C IV})/N(\text{H I}) > 0.015$: metal-rich absorbers.

There are 18 C IV-only type 1 components, $11.8 < \log N(\text{C IV}) < 13.8$, grouped in 8 C IV-H I systems.

Finally, a few absorbers with O VI blended with strong Lyman lines, and thus with uncertain values of $N(\text{O VI})$, are labelled type 2.

These different classes of absorbers are shown in figure 1. About 70% of the O VI+C IV-only type 1 absorbers have weak associated H I lines, $\log N(\text{H I}) < 13.6$, and the type 0 and type 1 O VI absorbers span roughly the same $N(\text{O VI})$ range. This demonstrates the importance of searching for O VI systems whatever the strength of their associated H I absorption.

Examples of type 1 absorbers are given in figure 2. The proximity in velocity space of a strong Ly- α system to a type 1 absorber is investigated in § 5.1. Examples of types 0 & 2 O VI absorbers and C IV-only type 1 absorbers are given in figures 3 and 4, respectively.

3. Abundances

3.1. O VI line widths

The histogram of O VI line widths is shown in figure 5. There are 81, 39 and 16 O VI components for the types 0, 1 and 2 absorbers, respectively. The bulk of the b distributions of the types 0 and 1 overlap, but not their high velocity tails. A Kolmogorov-Smirnov test shows that these distributions indeed differ at the 98% confidence level. It should be stressed that among the broader absorbers, $b > 16 \text{ km s}^{-1}$, most components are blends of several O VI lines within a velocity range of a few tens of km s^{-1} . Very few individual components are unambiguously broad.

Close to half (43%) of the O VI absorbers have line widths $b < 12 \text{ km s}^{-1}$. This confirms the results previously found with smaller O VI samples. The implied temperatures, $T < 1.4 \times 10^5 \text{ K}$, as also found for the non-saturated associated Lyman lines, are too low for O VI to be produced by collisional ionization even for abundances close to solar. We will thus assume that photoionization is the dominant ionization process, but will also consider simple cases where there is additional collisional heating of the gas, possibly through shocks.

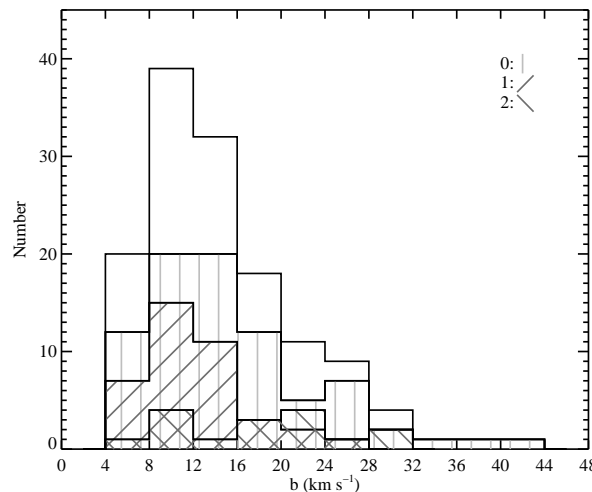


Figure 5. Distribution of the O VI line widths with the totals outlined.

3.2. Abundances under the assumption of photoionization

Following previous discussions on constraints of the spectral energy distribution of the ionizing background flux (e.g. Bergeron *et al.* 2002; Carswell *et al.* 2002; Telfer *et al.* 2002), we select a hard UV metagalactic flux (Haardt & Madau 1996) to derive the gas ionization level. We used the CLOUDY v94.0 code (Ferland *et al.* 1998) to estimate ionic column density ratios as a function of the ionization parameter, $U \equiv n_\nu/n_{\text{H}}$, and assumed solar relative abundances (Anders & Grevesse 1989). For each system, the value of U is fixed by the observed ionic ratio $\text{N(O VI)}/\text{N(C IV)}$ which is applicable only if O VI and C IV are in the same phase. This should be the case for most absorbers as Si IV is not detected, except in a few systems with large $\text{N(H I)} (> 10^{15} \text{ cm}^{-2})$. The observed range of $\text{N(O VI)}/\text{N(C IV)}$ implies $-1.4 \leq \log U \leq -0.4$, thus an ionization ratio $0.09 \leq \text{O VI/O} \leq 0.21$.

The distributions of the derived oxygen abundances are presented in figure 6 for the 31, 14 and 6 O VI systems of type 0, 1 and 2, respectively. Contrary to the distribution of $b(\text{O VI})$ shown above, there is very little overlap between the [O/H] distributions of the types 0 and 1 populations. This further suggests that they are indeed two distinct populations. The type 2 [O/H] distribution spans a small range in between those of the other two populations.

3.3. Abundances under the assumption of other ionization processes

To confirm the difference in metallicity between the type 0 (population tracing the IGM) and type 1 (population tracing highly metal-enriched sites) absorbers, we investigate

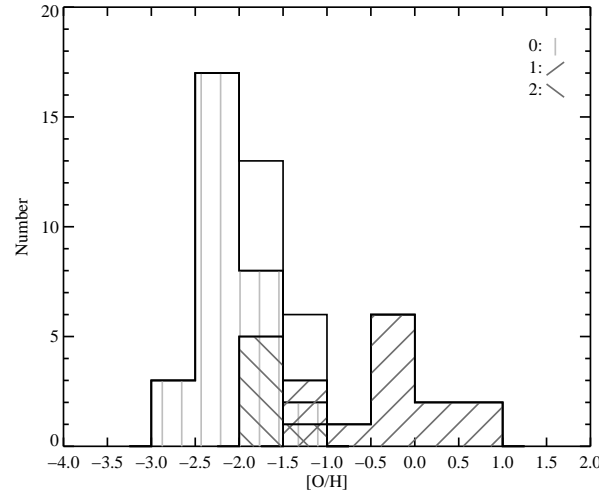


Figure 6. Distribution of the oxygen abundance in the photoionization case. The [O/H] median values for the types 0, 1 and 2 populations are -2.07 , -0.33 and -1.56 , respectively.

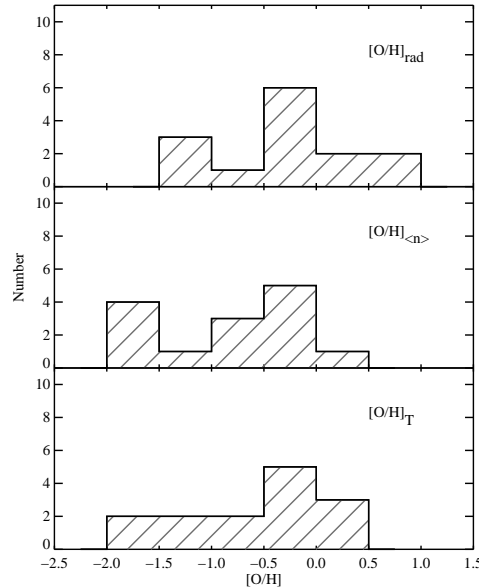


Figure 7. Distributions of the oxygen abundance for the type 1 population under various ionization conditions: (1) pure photoionization case (top panel), (2) constant gas density (middle panel), (3) photoionization plus temperature fixed by $b(\text{O VI})$ (bottom panel). The [O/H] median values for the cases 1, 2 and 3 are -0.33 , -0.80 and -0.35 , respectively.

whether other ionization conditions could yield much lower abundances for the type 1 population.

First, we consider a gas phase of constant density, ρ , thus a single value of the ionization parameter. We select an overdensity $\delta \equiv (\rho/\bar{\rho}) \approx 10$ at $z \approx 2.2$ which is within the range of values found in the previous O VI surveys. This yields $\log U = -0.5$, thus an ionization

ratio $O\,\text{VI}/O = 0.16$. In a large fraction of these cases, $O\,\text{VI}$ and $\text{C}\,\text{IV}$ do not trace the same phase.

Secondly, we reconsider photoionization by a hard UV background flux but now with the gas temperature derived from the b value of the main $O\,\text{VI}$ component of each system. This is to account for possible additional shock heating. The value of U is still derived from the observed $N(O\,\text{VI})/N(\text{C}\,\text{IV})$ ionic ratio. There is no solution for absorbers with $T > 2.0 \times 10^5$ K, or $b > 14 \text{ km s}^{-1}$, implying that at these higher temperatures $O\,\text{VI}$ and $\text{C}\,\text{IV}$ are not co-spatial. However, for the type 1 systems, the main $O\,\text{VI}$ component is always narrower than 14 km s^{-1} except in the case of one $O\,\text{VI}$ doublet blended with Lyman lines.

Together with the case of pure photoionization, the distributions of the oxygen abundances estimated in the above two cases are shown in figure 7. Although the values of $[\text{O}/\text{H}]$ are somewhat lower under the new ionization conditions, they remain far higher than those of the type 0 population. This confirms that the types 0 and 1 $O\,\text{VI}$ absorbers trace markedly different populations.

4. Contribution of the $O\,\text{VI}$ absorbers to the cosmic baryon density

4.1. Column density distribution

The column density distribution, $f(N)$, of $O\,\text{VI}$ absorbers per unit redshift path per unit column density can be written:

$$f(N) = \{n/(\Delta N \sum \Delta X)\}, \quad (4.1)$$

where n is the number of $O\,\text{VI}$ absorbers in a column density bin ΔN centered on N for a sample of quasars with total redshift path $\sum \Delta X$. For our adopted cosmology, the redshift path is defined as:

$$dX \equiv (1+z)^2 \{\Omega_\Lambda + \Omega_m(1+z)^3\}^{-0.5} dz, \quad (4.2)$$

$$\text{or } dX/dz \cong \{(1+z)/0.3\}^{0.5} \text{ when } z > 1.$$

The $O\,\text{VI}$ column density distribution is shown in figure 8. It can be seen that the present data become incomplete below a column density of $\sim 1 \times 10^{13} \text{ cm}^{-2}$ and that sample variance may be important at column densities larger than $\sim 2 \times 10^{14} \text{ cm}^{-2}$. In between these limits, a power-law fit ($f(N) \propto N^{-\alpha}$) gives $\alpha \simeq 1.7$. To estimate the uncertainty in α , we shift the ΔN bins by 0.1 dex and derive new power-law fits. This yields $\alpha = 1.71 \pm 0.48$ and a normalization of $f(N) = 2.3 \times 10^{-13}$ at $\log N(O\,\text{VI}) = 13.5$, with a $\sim 30\%$ uncertainty.

The value of the power-law index is similar to that obtained from $\text{C}\,\text{IV}$ samples, $\alpha(\text{C}\,\text{IV}) \simeq 1.8$, such as those drawn from the *VLT-UVES* Large Programme at $\bar{z}(\text{C}\,\text{IV}) = 2.16$ (Scappapietra *et al.* 2005) or from *Keck-HIRES* data at higher redshift (Songaila 2001). The power-law fit of the latter (corrected for the different adopted cosmological parameters) is also shown in figure 8. At $N(O\,\text{VI}) = N(\text{C}\,\text{IV}) = 10^{13.5} \text{ cm}^{-2}$, the value of $f(N)$ for $O\,\text{VI}$ absorbers is nearly a factor of ten larger than that for $\text{C}\,\text{IV}$ absorbers.

4.2. Number density

We use the power-law fit to $f(N)$ for the $O\,\text{VI}$ population to estimate the number density per unit z of $O\,\text{VI}$ absorbers:

$$dn/dz = (dX/dz) \int f(N) dN. \quad (4.3)$$

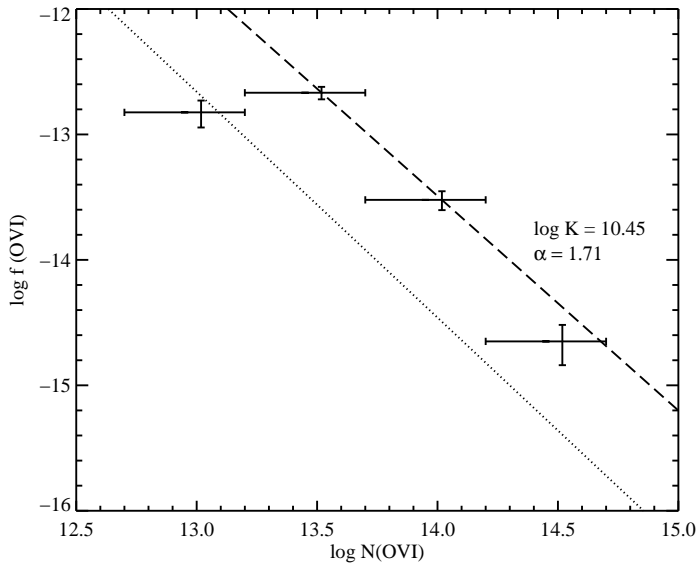


Figure 8. Column density distribution of O VI absorbers. The dashed line is the fit to our data in the column density range $13.0 < \log N(\text{O VI}) < 14.3$ (see text). The dotted line is the fit to the column density distribution of C IV absorbers given by Songaila (2001).

We select conservative $N(\text{O VI})$ limits of 10^{13} and 10^{15} cm^{-2} , a range that is not drastically affected by incompleteness or sample variance. Adopting the fit with $\alpha = 1.71$, we then get $dn/dz = 74$ at $\bar{z} = 2.3$. Taking into account the range of possible values of the power-law index and normalization factor of $f(N)$, we obtain $66 < dn/dz < 106$.

At low redshift, $\bar{z} = 0.1$, surveys with *FUSE* and *HST* give $dn/dz \approx 13$ for a rest-equivalent width limit of $w_{r,\text{min}} = 50 \text{ m}\text{\AA}$, or $\log N(\text{O VI}) = 13.60$ in the optically thin case (see Sembach *et al.* 2004). For this column density limit, we get $dn/dz \approx 26$ at $\bar{z} = 2.3$, whereas we expect a somewhat higher value, $dn/dz \approx 36$, in the case of an unevolving O VI population. However, comparison between the values of dn/dz at $\bar{z} = 0.1$ and 2.3 is not straightforward as O VI absorbers may trace different populations at low and high redshift.

4.3. Cosmic density of O VI absorbers

The O VI cosmic density can be expressed as a mass fraction relative to the critical density, ρ_{crit} . It can be estimated either from the individual, observed O VI column densities or using the power-law fit to $f(N)$ of O VI absorbers to correct for incompleteness.

4.3.1. Observed O VI cosmic density

The mean cosmic density of a given ion can be expressed as:

$$\Omega_{\text{b,ion}} = \{H_0 m_{\text{ion}} / c \rho_{\text{crit}}\} \left\{ \sum N_{\text{ion}} / \sum \Delta X \right\} = 2.20 \times 10^{-22} \left\{ \sum N_{\text{ion}} / \sum \Delta X \right\}, \quad (4.4)$$

where H_0 is the Hubble constant, m_{ion} and $\sum N_{\text{ion}}$ the atomic mass and the sum of the column densities of the given ion, respectively, and $\sum \Delta X$ the total redshift path. For our O VI sample, we obtain $\Omega_{\text{b}}(\text{O VI}) = 1.51 \times 10^{-7}$, a value higher than previous estimates by a factor 1.3 (Simcoe *et al.* 2004: sample restricted to O VI systems with strong, associated H I absorption [see § 2.1]) and 1.8 (Carswell *et al.* 2002: two sightlines, none with very

strong O VI absorbers). The contribution of the O VI type 1 population to $\Omega_b(\text{O VI})$ is 35%.

4.3.2. O VI cosmic density corrected for incompleteness

The mean cosmic density of O VI ions can also be written as:

$$\Omega_b = 2.20 \times 10^{-22} \int N f(N) dN \quad (4.5)$$

Using our fit with $\alpha = 1.71$ and the same $N(\text{O VI})$ limits as in § 4.2, we get $\Omega_b(\text{O VI}) \approx 3.5 \times 10^{-7}$, thus an incompleteness correction factor of 2.3 at $\bar{z} = 2.3$. The uncertainty in the power-law fit of $f(N)$ leads to values in the range $2.6 \times 10^{-7} < \Omega_b(\text{O VI}) < 6.7 \times 10^{-7}$.

To estimate the mean cosmic density of oxygen, $\Omega_b(\text{O})$, we use the O VI mean ionization level obtained in the pure photoionization case, $\langle \text{O VI}/\text{O} \rangle = 0.15$ (see § 3.2). Under the other ionization conditions investigated in § 3.3, this ratio is either similar or smaller. We then get $\Omega_b(\text{O}) \approx (2.3 \pm 0.6) \times 10^{-6}$.

Using the solar oxygen abundance given by Anders & Grevesse (1989), yields:

$$\log (\Omega_b(\text{O})/\Omega_b(\text{O})_\odot) = -2.22.$$

This result demands attention for the two following reasons: (1) the above value is close to the median of [O/H] found for the O VI type 0 absorbers (IGM), [O/H] = -2.07 , but well below that of the O VI type 1 absorbers (metal-enriched sites), [O/H] = -0.33 (see figures 6 and 7), and (2) it is smaller than the mean metal enrichment of the IGM by star-forming galaxies at $z \sim 2.5$ (Z^{SF}) by a factor of about 3.7 and 6.6 when adopting the values of $Z^{\text{SF}} \approx 1/45$ and $1/25$ solar as given by Ferrara *et al.* (2005) and Pettini (1999), respectively. Consequently, there is still a shortfall of observed metals as compared to those produced by LBGs, but about a factor three smaller than previously thought.

Our sample contains very few cases of unambiguously broad O VI doublets ($b > 16 \text{ km s}^{-1}$) which could trace hotter parts ($T > 2.5 \times 10^5 \text{ K}$) of metal-rich sites. However, if most of the gas in these sites is at even higher temperatures, oxygen will then mainly be in the form of O VII and O VIII ions and not detectable with present-day X-ray satellites.

5. Origin of the O VI absorbers

5.1. Nearest strong H I absorption system

From a pixel analysis of *VLT-UVES* Large Programme quasar spectra, Aracil *et al.* (2004) found that weak O VI absorption associated with weak H I absorption ($0.2 < \tau(\text{Ly-}\alpha) < 1$ or $12.9 < \log N(\text{H I}) < 13.6$ for $b(\text{H I}) = 30 \text{ km s}^{-1}$) is predominantly detected in the vicinity ($\Delta v \leq 300 \text{ km s}^{-1}$) of strong H I absorption ($\tau(\text{Ly-}\alpha) > 4$). These authors suggested that the O VI absorption arising in regions spatially close to strong Ly- α absorption may be part of outflows from overdense regions.

The O VI type 1 population from our study should exhibit the same property as the weak O VI absorptions analyzed with the pixel analysis method, since there is an overlap in their $N(\text{H I})$ range. The distribution of Δv between O VI or C IV-only type 1 systems and the nearest strong Ly- α system ($\tau(\text{Ly-}\alpha) > 4$) is presented in figure 9. For the few cases of an O VI doublet associated with a saturated Ly- α line, Δv is nul. It should be noted that all C IV-only type 1 systems have unsaturated, associated Ly- α lines.

Among the O VI and C IV-only type 1 systems, 64% and 63%, respectively, have a strong Ly- α system at $\Delta v < 450 \text{ km s}^{-1}$. Results from both the pixel analysis method of weak O VI systems ($\log \tau(\text{O VI}) \sim -1.35$) and the study of individual O VI absorbers suggest a link to gas outflows.

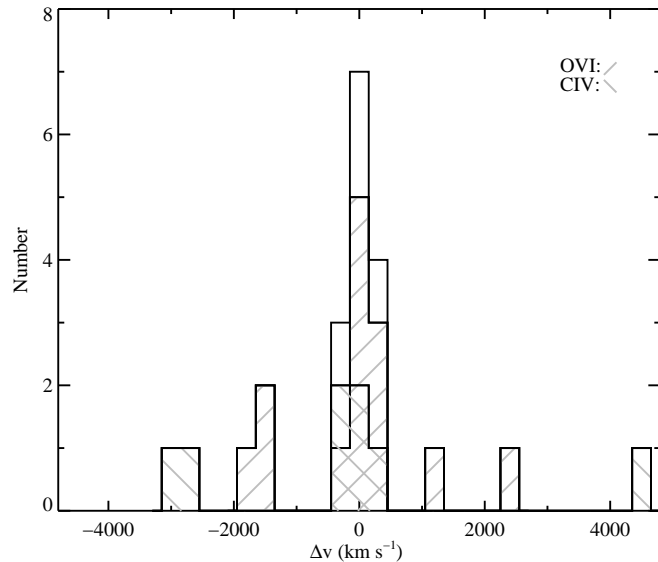


Figure 9. Distribution of the velocity difference between type 1 systems and the nearest strong Ly- α system, with the totals outlined.

5.2. Gas density of the O VI absorbers

The gas overdensity of the O VI absorbers is estimated for two cases: photoionization by a hard UV metagalactic flux and hydrostatic equilibrium (Schaye 2001).

In the photoionization case U is fixed by the O VI/C IV ionic ratio, assuming a relative O/C solar abundance. In the range $2.0 < z < 2.5$, the adopted hydrogen photoionization rate is $\Gamma(\text{H I}) \approx 1.5 \times 10^{-12} \text{ s}^{-1}$. Using the mean baryon density at each $z(\text{O VI})$, we get:

$$\delta(U) \approx 4.0 U^{-1} ([1+z]/3)^{-3}. \quad (5.1)$$

The results are shown in figure 10 for the different types of O VI absorbers. The median values of $\delta(U)$ for the type 0 (metal-poor) and type 1 (metal-rich) populations are equal, $\delta(U) = 22$, and that of the type 2 population is $\sim 40\%$ smaller. A Kolmogorov-Smirnov test shows that the types 0 and 1 populations have the same $\delta(U)$ distribution at the 97% confidence level.

For the hydrostatic equilibrium case (Schaye 2001: equation (8)), we assume a gas temperature $T = 4 \times 10^4 \text{ K}$ and the same photoionization rate as above. This gives:

$$\delta(G) = 3.7 \times 10^{-9} \text{ N}(\text{H I})^{2/3} ([1+z]/3)^{-3}. \quad (5.2)$$

The results are presented in figure 11. Contrary to the photoionization case, there is a marked difference between the types 0 and 1 populations. The median values of $\delta(G)$ are 41 and 4.6 for the type 0 and type 1 absorbers, respectively, and that for the type 2 absorbers is 8.3. Moreover, the values of $\delta(G)$ for $\sim 80\%$ of the type 1 population ($\log \delta(G) < 1.1$) do not overlap with those obtained for the type 0 population.

We now compare in figure 12 the values of $\delta(U)$ and $\delta(G)$ to check the validity of the assumption of hydrostatic equilibrium. For the type 0 absorbers, a Spearman rank correlation test shows that $\delta(G)$ and $\delta(U)$ are correlated at a $>99\%$ confidence level. The mean value of their $\delta(G)/\delta(U)$ overdensity ratio is close to 2.0. It cannot be substantially

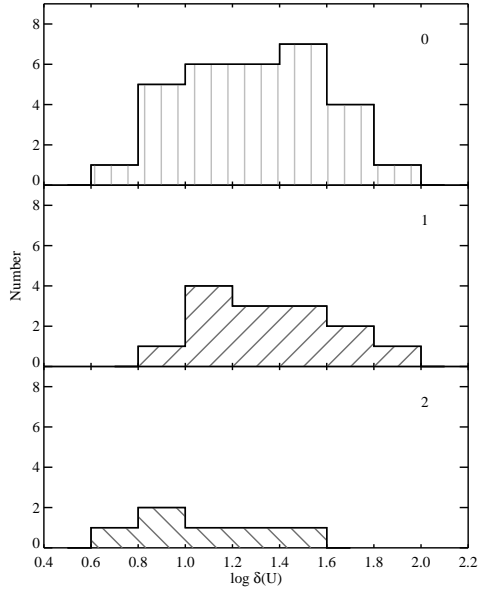


Figure 10. Distribution of the O VI absorber overdensity in the photoionization case.

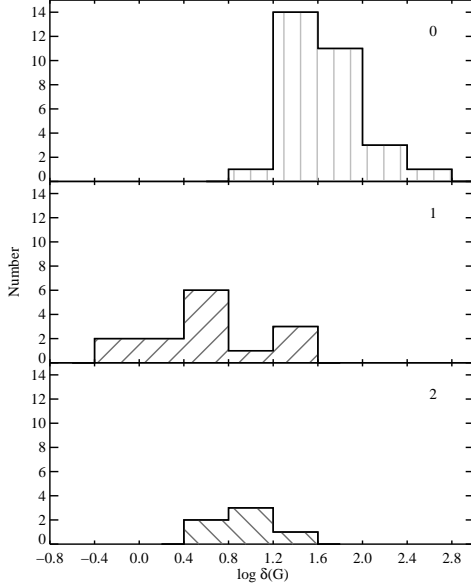


Figure 11. Distribution of the O VI absorber overdensity in the hydrostatic equilibrium case.

decreased as its dependence on $\Gamma(\text{H I})$, mass fraction in gas and T is small ($\delta(G)/\delta(U) \propto T^{0.17}\Gamma(\text{H I})^{-1/3} (\Omega_b/\Omega_m)^{-1/3}$). Therefore, this departure of $\delta(G)/\delta(U)$ from unity may suggest that a fraction of the observed H I is not in the O VI phase. Nevertheless, the correlation between $\delta(G)$ and $\delta(U)$ suggests that the O VI type 0 population is roughly in hydrostatic equilibrium. For the type 1 absorbers, $\delta(G)$ and $\delta(U)$ are totally uncorrelated which implies that hydrostatic equilibrium is not a valid assumption for this population:

low H I column density absorbers do not trace low density regions of the IGM. This further supports that the metal-rich and metal-poor absorbers trace different populations.

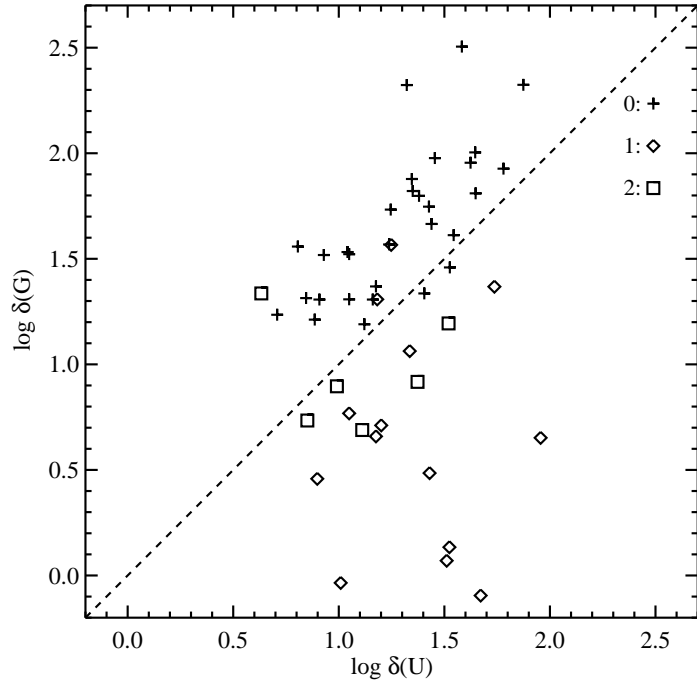


Figure 12. Comparison of the O VI absorber overdensities in the photoionization versus hydrostatic equilibrium cases.

6. Conclusions and prospectives

Our large *VLT-UVES* sample of 136 O VI absorbers at $\bar{z} = 2.28$ towards ten quasars enables a study of the highly ionized phase of the IGM, in particular its metal enrichment and contribution to the cosmic baryon density.

Previous O VI studies at high z have uncovered a few systems with high [O/H] (> -1.0) abundances, motivating us to fully investigate this class of metal-rich absorbers. Because those systems already identified have low H I column densities (Bergeron *et al.* 2002; Carswell *et al.* 2002), our sample includes all detected O VI systems whatever the strength of their associated H I absorption. In contrast, the survey by Simcoe *et al.* (2004) only includes systems with $N(\text{H I}) > 10^{13.6} \text{ cm}^{-2}$. We restrict our sample to absorbers with both lines of the O VI doublet clearly detected or, if partially blended, enough unambiguous structure to allow for deblending from Lyman lines.

Since nearly half of the O VI absorbers have small line widths, $b < 12 \text{ km s}^{-1}$ or $T < 1.4 \times 10^5 \text{ K}$, photoionization must be the dominant ionization process. We thus introduce an observational identification criterium to separate the classes of metal-poor (type 0) and metal-rich (type 1) absorbers. Selecting a hard UV background flux (see Bergeron *et al.* 2002; Carswell *et al.* 2002 ; Telfer *et al.* 2002) and assuming a 0.1 solar metallicity yields a column density ratio $N(\text{O VI})/N(\text{C IV}) < 0.25$ and > 0.25 for the type 0 and type 1 populations, respectively.

The bulk of the b distributions of these two O VI populations are similar except at the highest velocities. However, we stress that very few individual components are unambiguously broad, a result of blending for complex, multiple systems and limited S/N (~ 30 -40) in the O VI range.

The cosmic oxygen abundance is derived under the assumptions of photoionization, coexistence of O VI and C IV in the same phase, and a solar O/C relative abundance. The overall [O/H] distribution is clearly bimodal with median values of [O/H] equal to -2.05 and -0.33 for the type 0 and type 1 populations, respectively. This is not a consequence of a strong difference in ionization levels between the two types of O VI absorbers. All of the type 1 O VI systems and all but two of the type 0 systems have associated C IV absorption (detection limit of $N(C IV) \approx 1 \times 10^{12} \text{ cm}^{-2}$). Their $N(O VI)/N(C IV)$ distributions, which cover about two orders of magnitude, are similar with median values both close to 10. A high metallicity (median [O/H] > -1.0) for the type 1 population is still found under different ionization conditions: photoionization together with either a gas phase of constant density (overdensity $\delta = 10$ at $z = 2.2$) or a temperature fixed by the line width of the main O VI component of each system (always $< 14 \text{ km s}^{-1}$).

The $N(N V)/N(O VI)$ ratio cannot be used to constrain the ionization level of the O VI phase because the N/O relative abundance departs from the solar value. In most O VI absorbers, the N V doublet is weak or undetected and the nitrogen abundance relative to oxygen is usually well below solar (Bergeron *et al.* 2002). For a very few O VI systems, the strength of the N V absorption is similar to those of C IV and O VI and the nitrogen abundance may be enhanced relative to that of oxygen (Carswell *et al.* 2002), as also observed in quasar associated systems (e.g. Hamann *et al.* 2000). In our type 1 O VI sample, associated N V absorption is either absent or very weak, except in one case already reported by Bergeron *et al.* (2002). This absorber at $z = 2.352$ in Q 0329–385 was labelled as “intrinsic” by these authors because its properties are typical of those of associated systems, even though it is at 6200 km s^{-1} from the quasar emission redshift.

Our O VI sample is large enough to derive the first estimate of the O VI column density distribution, although incompleteness becomes evident at $N(O VI) \lesssim 1 \times 10^{13} \text{ cm}^{-2}$ and sample variance may be important at $N(O VI) \gtrsim 2 \times 10^{14} \text{ cm}^{-2}$. A power-law fit, $f(N) \propto N^{-\alpha}$, yields $\alpha \approx 1.7 \pm 0.5$, a value similar to that found for C IV samples, $\alpha(C IV) \simeq 1.8$ (Songaila 2001; Scannapieco *et al.* 2005). In contrast, the normalization factor, $f(N) = 2.3 \times 10^{-13}$ (with an uncertainty of $\sim 30\%$) at $N(O VI) = 10^{13.5} \text{ cm}^{-2}$, is about ten times larger than that of C IV absorbers. We aim to better constrain $f(N)$, particularly at large O VI column densities, by analyzing a larger number of sightlines in a future paper. There we will also include blended O VI components associated with C IV absorption.

We use the fit to $f(N)$ in a conservative N(O VI) range, 10^{13} - 10^{15} cm^{-2} , to estimate the number density per unit z of O VI absorbers as well as their cosmic density. This is a first step for correcting dn/dz and $\Omega_b(O VI)$ from incompleteness and sample variance. We find $dn/dz = 74 \pm 32$. Selecting an integration range as wide as is usually adopted for C IV (10^{12} - 10^{16} cm^{-2}) would yield a larger value of dn/dz (and of $\Omega_b(O VI)$) but the uncertainty on the result would then be far too large. In the case of an unevolving population and a column density lower limit equal to that of low $\bar{z} = 0.1$ O VI surveys, that is $N(O VI)_{\min} = 10^{13.6} \text{ cm}^{-2}$ or $w_{r,\min} = 50 \text{ m}\text{\AA}$ (see e.g. Sembach *et al.* 2004), the expected value of dn/dz at $\bar{z} = 2.3$ derived from the low z samples is 36 (assuming a 0.1 solar metallicity and an ionic fraction O VI/O = 0.2), whereas that obtained from our $f(N)$ distribution equals 26. The suggested decline of dn/dz with z is not straightforward to interpret as the O VI absorbers may trace different populations at low and high z .

The O VI cosmic density estimated from the individual, observed column densities is $\Omega_b(O VI) \approx 1.5 \times 10^{-7}$, i.e. higher than previous estimates by a factor 1.3 (Simcoe *et al.*

2004) and 1.8 (Carswell *et al.* 2002). This increase is due to the high contribution (35%) of the type 1 population to $\Omega_b(\text{O VI})$. The value derived from the $f(N)$ distribution is 2.3 times larger: $\Omega_b(\text{O VI}) \approx (3.5 \pm 3.2) \times 10^{-7}$. This illustrates the effects of incompleteness and sample variance in our sample, even within the conservative N(O VI) range adopted. To get the element cosmic density, we use the mean ionic fraction obtained in the pure photoionization case, $\langle \text{O VI/O} \rangle = 0.15$, which yields $\Omega_b(\text{O}) \approx (2.3 \pm 2.1) \times 10^{-6}$.

Adopting the solar oxygen abundance given by Anders & Grevesse (1989), we get $\log(\Omega_b(\text{O})/\Omega_b(\text{O}_\odot)) = -2.22$. This value is well below that of the metal-rich population and also smaller than the metal enrichment of the IGM expected from high z star-forming galaxies, $\langle [\text{O}/\text{H}] \rangle \sim -1.40$ (Pettini 1999) or -1.65 (Ferrara *et al.* 2005). Although the problem of missing metals at high z (where previously an order of magnitude disparity was measured) is now less severe as a result of our O VI survey, there remains a shortfall of observed metals by about a factor of four as compared to those produced by star-forming galaxies.

Other properties of the type 1 O VI absorbers suggest a tight link to galactic halos. This population is predominantly detected in the vicinity ($\Delta v < 450 \text{ km s}^{-1}$) of strong H I systems ($\tau(\text{Ly-}\alpha) > 4$). This is also the case for C IV-only metal-rich absorbers (O VI doublet either outside the observing range, $z < 2.0$, or fully blended with saturated Lyman lines). In the photoionization case, the type 0 and type 1 O VI absorbers have the same gas overdensity distribution, with a median value $\delta(U) = 22$, but under the assumption of hydrostatic equilibrium the gas overdensity, $\delta(G)$, distributions of these two populations barely overlap. Moreover, the values of $\delta(U)$ and $\delta(G)$ are totally uncorrelated for the metal-rich population, whereas they are well correlated for the metal-poor population. Consequently, the assumption of hydrostatic equilibrium is not valid for the metal-rich O VI population: these absorbers do not trace low density regions of the IGM but rather gas outflows in the vicinity of active star-formation sites.

If most of the gas in the metal-rich sites is at high temperature ($T > 5 \times 10^5 \text{ K}$), as suggested by Pettini (1999), oxygen will mainly be in the form of O VII and O VIII ions and their signatures in the very soft X-ray range are not detectable with present-day X-ray satellites. For a phase at lower temperatures, $2 \times 10^5 < T < 5 \times 10^5 \text{ K}$, the O VI and H I species, but not C IV (ionic fraction $\text{C IV/C} < 10^{-2}$), should be detectable. We have begun to search for these absorbers with broad ($b > 50 \text{ km s}^{-1}$), weak Ly- α lines associated with semi-broad, weak O VI doublets ($b > 15 \text{ km s}^{-1}$). This is coupled to a statistical analysis of the Ly- α forest in simulated spectra (in progress).

We also plan to acquire deep, multi-band images of the quasar fields with several metal-rich O VI absorbers. If this population does indeed trace hot galactic halos, we expect to find a strong correlation with star-forming galaxies. Using these images together with spectroscopic follow-up of the associated galaxies may help clarify the ejection mechanism(s) responsible for the metal-pollution of galactic halos and the surrounding IGM.

Acknowledgements

S. Herbert-Fort is supported by the EU under the Marie Curie Early Stage Training programme EARA-EST.

References

- Anders, E. & Grevesse, N. 1989, *Geochim. Cosmochim. Acta* 53, 197
- Aracil, B., Petitjean, P., Pichon, C. & Bergeron, J. 2004, *A&A* 419, 811
- Bergeron, J., Aracil, B., Petitjean, P. & Pichon, C. 2002, *A&A* 396, L11

Bertone, S., Stoehr, F. & White, S. 2005, *MNRAS* 359, 1216

Carswell, B., Schaye, J., & Kim, T.-S. 2002, *ApJ* 578, 43

Cen, R. & Ostriker, J.P. 1999, *ApJ* 514, 1

Davé, R., Cen, R., Ostriker, J.P., Bryan, G.L., Hernquist, L., Katz, N., Weinberg, D.H., Norman, M.L. & O'Shea, B. 2001, *ApJ* 552, 473

Ferland, G.J., Korista, K.T., Verner, D.A., Ferguson, J.W., Kingdon, J.B. & Verner, E.M. 1998, *PASP* 110, 761

Ferrara, A., Scannapieco, E. & Bergeron, J. 2005 preprint

Fukugita, M., Hogan, C.J. & Peebles, P.J.E. 1998, *ApJ* 503, 518

Haardt, F. & Madau, P. 1996, *ApJ* 461, 20

Hamann, F., Netzer, H. & Shields, J.C. 2000, *ApJ* 536, 101

Nicastro, F., Elvis, M., Fiore, F. & Mathur, S. 2005a, astro-ph/0501126

Nicastro, F., Mathur, S., Elvis, M., Drake, J., Fang, T., Fruscione, A., Krongold, Y., Marshall, H., Williams, R. & Zezas, A. 2005b, *Nature* 433, 495

Pettini, M. 1999, astro-ph/9902173

Richter, P., Savage, B.D., Tripp, T.M. & Sembach, K.R. 2004, *ApJS* 153, 165

Savage, B.D., Sembach, K.R., Tripp, T.M. & Richter, P. 2002, *ApJ* 564, 631

Schaye, J. 2001, *ApJ* 559, 507

Scannapieco, E., Pichon, C., Aracil, B., Petitjean, P., Thacker, R.J., Pogosyan, D., Bergeron, J. & Couchman, H.M.P. 2005, astro-ph/0503001

Sembach, K.R., Tripp, T.M., Savage, B.D. & Richter, P. 2004, *ApJS* 155, 351

Simcoe, R.A., Sargent, W.L.W. & Rauch, M. 2002, *ApJ* 578, 737

Simcoe, R.A., Sargent, W.L.W. & Rauch, M. 2004, *ApJ* 606, 115

Songaila, A. 2001, *ApJ* 561, L153

Telfer, R.C., Kriss, G.A., Zheng, W., Davidsen, A.F. & Tytler, D. 2002, *ApJ* 579, 500